94. Axially Dissymmetric Diphosphines in the Biphenyl Series: Crystal Structures of Three New Group-VIII Metal Complexes of (6,6′-Dimethyl-1,1′-biphenyl-2,2′-diyl)bis(diphenylphosphine) (= biphemp)

by **Andreas Knierzinger*** and **Peter Schönholzer**

Department of Vitamin and Nutrition Research
and Central Research Units, *F. Hoffmann La-Roche AG*, CH-4002 Basel

Dedicated to Prof. *Erich Ziegler* on the occasion of his 80th birthday

(20.III.92)

(6,6′-Dimethyl-1,1′-biphenyl-2,2′-diyl)bis(diphenylphosphine) (= biphemp) reacts with allylmetal halides to yield complexes **1**–**3** which were transformed into the corresponding perchlorates **4**–**6**. The molecular structures of **4**–**6** were determined by X-ray analyses.

1. Introduction. – The discovery of bidendate, axially dissymmetric bis(triarylphosphine) ligands ('binap', 'biphemp') led to significant advances in asymmetric catalysis. Rhodium and ruthenium complexes of such phosphines were found to be extremely effective catalysts for various asymmetric hydrogenations and isomerizations [1] [2]. Previous contributions from our laboratories dealt with the synthesis of biphemp (including a number of derivatives) [3] [4], the preparation of the corresponding Rh and Ru complexes [5], and their application to the synthesis of various acyclic terpene intermediates. Our interest in Pd, Pt, and Ni complexes of biphemp arose from their possible utilization in the total synthesis of (*R*,*R*,*R*)-α-tocopherol. Specifically, we wanted to use them for the installment of the quaternary asymmetric center at the chroman ring of tocopherol by an allylic substitution reaction. The results of this work were recently disclosed [6].

In the course of these studies, we came to know that the optimization of a catalytic reaction requires specific catalyst tailoring for each particular application. Presently, this is largely achieved by intuitively conceived changes of the ligand-substitution pattern. Future developments in this area will most likely involve a more rational design of modified or entirely new ligands. Accurate structural data form the basis of any such effort. We, therefore, wish to communicate the X-ray analyses of the three new complexes **4**–**6** incorporating the biphemp ligand.

2. Results. – The complexes **4**–**6** were prepared from the known [7] bridged allylmetal halides. These halide complexes dissociated in the presence of biphemp, and the corresponding monomeric species were trapped by the phosphine ligand to produce the new complexes **1**–**3**. Subsequent anion exchange with $LiClO_4$ yielded the desired salts **4**–**6** as colorless, perfectly air-stable powders. This anion exchange was preferably conducted *in situ* to avoid losses during the isolation of the somewhat less stable complexes **1**–**3**. In fact, it was not possible to obtain **3** in pure form. Unprotected solutions of **1** and **2** quickly

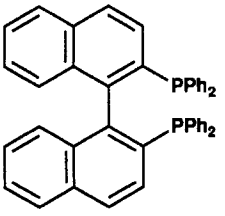

binap

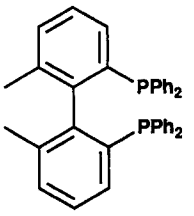

biphemp

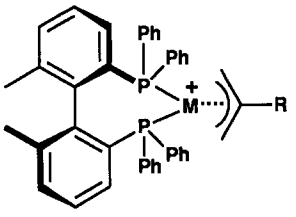

X⁻

1 M=Pd, R=H, X=Cl
2 M=Pt, R=H, X=Cl
3 M=Ni, R=Me, X=Br
4 M=Pd, R=H, X=ClO_4
5 M=Pt, R=H, X=ClO_4
6 M=Ni, R=Me, X=ClO_4

became yellow to orange, and NMR examination of these materials confirmed substantial decomposition. The *in situ* protocol, however, produced **4**–**6** in analytically pure form.

Crystals for X-ray analysis were grown by slow evaporation of solvent at room temperature. Good quality crystals of **4** and **5** formed readily, while only marginal quality could be achieved for **6**. The crystals are built up of discrete ions. The ClO_4^- ion is disordered in all cases and merely serves to fill the voids left between the cations. No extra solvent molecules are incorporated in the lattices. Complexes **4** and **5** are crystallographically isomorphous (r.m.s.d. of the cations, 0.06 Å). Their cations are stacked along an axis roughly perpendicular to the aryl–aryl bond and experience extensive intermolecular *van-der-Waals* contacts (mostly of the edge-to-face type) between their aromatic rings. The (unsubstituted) allyl groups are snugly enfolded by the Ph–P–Ph moiety of a neighboring cation. The extra Me group of the $CH_2C(Me)CH_2$ moiety of **6** can not be accommodated in such an arrangement, and hence, a different packing becomes preferred for this complex. Cations of **6** are stacked along an axis parallel rather than perpendicular to the aryl–aryl bond. This latter stacking causes an increased deformation along the biaryl backbone and is responsible for the somewhat less symmetrical appearance of **6** (r.m.s.d. of the cations **5**/**6**, 0.34 Å). The methylallyl group in **6** then appears near one of the aromatic Me substituents.

Though known from the synthesis, the absolute configurations of the complexes were determined *via* the anomalous scattering by the respective heavy atoms. They were confirmed to be (*R*) in all cases. Stereoscopic representations of the structures are given in *Figs. 1–3*. Selected geometrical parameters are collected in *Table 1* (atom numbering according to *Fig. 4*).

The complexes exhibit distorted square-planar coordination geometry as defined by the two P-atoms and the two terminal allylic C-atoms. The metal resides almost perfectly in the mean coordination plane. The allylic ligand is clearly η^3-bonded, as evidenced by the nearly identical metal-C distances within each structure. The central C-atom of the allyl moiety is disordered in two positions in the Pd and Pt complexes **4** and **5** (see C(40a) and C(40b)). The calculated occupation factors are 0.45 and 0.55 (**4**) and 0.5 and 0.5 (**5**). Both positions are roughly equally distant from the coordination plane (0.5 Å in **4**, and 0.6 Å in **5**) and slightly closer to the metal atom than the terminal C-atoms. This type of

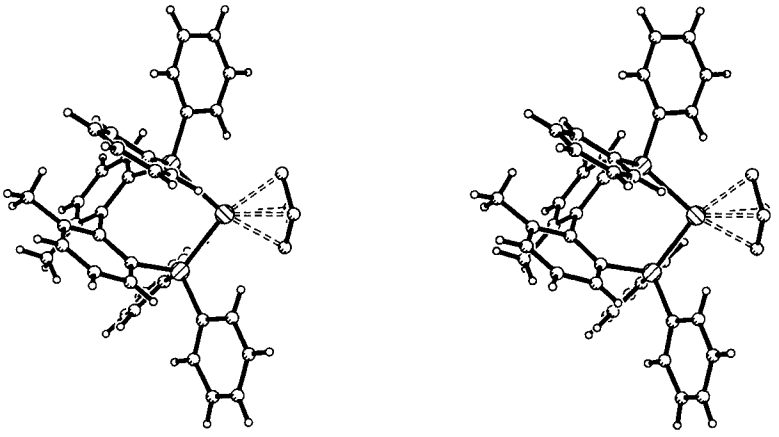

Fig. 1. *Stereoscopic representation of [Pd{(R)-biphemp}(allyl)]*$^+$ (cation of **4**)

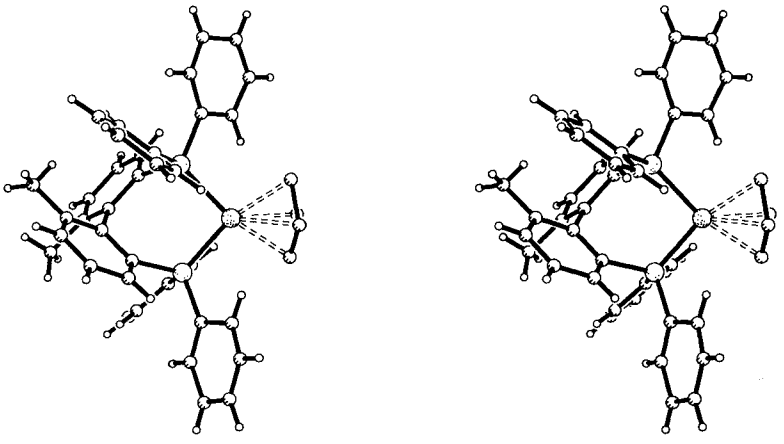

Fig. 2. *Stereoscopic representation of [Pt{(R)-biphemp}(allyl)]*$^+$ (cation of **5**)

disorder was frequently reported for unsubstituted π-allyl complexes [8]. It is absent in the Ni complex **6**. The central C-atom of the methylallyl moiety of **6** is slightly farther from the metal atom than its neighbors, resulting in an angle of 117° between the coordination plane and the plane of the allylic ligand. The Me group of methylallyl does not lie in the latter plane but is tilted slightly (0.31 Å) towards the metal. As in most published structures of π-allyl complexes, the C–C bond lengths of the allyl ligand are not identical. In the present cases, this is probably due to the relatively high thermal mobilities in this part of the molecules, rather than to genuine asymmetry or to crystal-packing effects. For **4** and **5**, these lengths are well within the range of reported [8] values and represent essentially double bonds with some single-bond character. Untypically short C–C bonds (1.27(3) and 1.34(4) Å) are, however, observed in the methylallyl ligand of **6**. The metal–P bond lengths decrease in going from Pd (2.32(0.2), 2.30(0.2) Å) *via* Pt

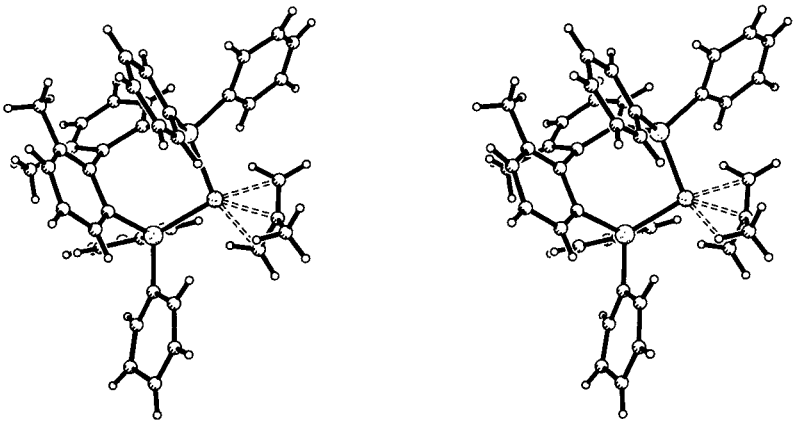

Fig. 3. *Stereoscopic representation of [Ni{(R)-biphemp}(2-methylallyl)]$^+$* (cation of **6**)

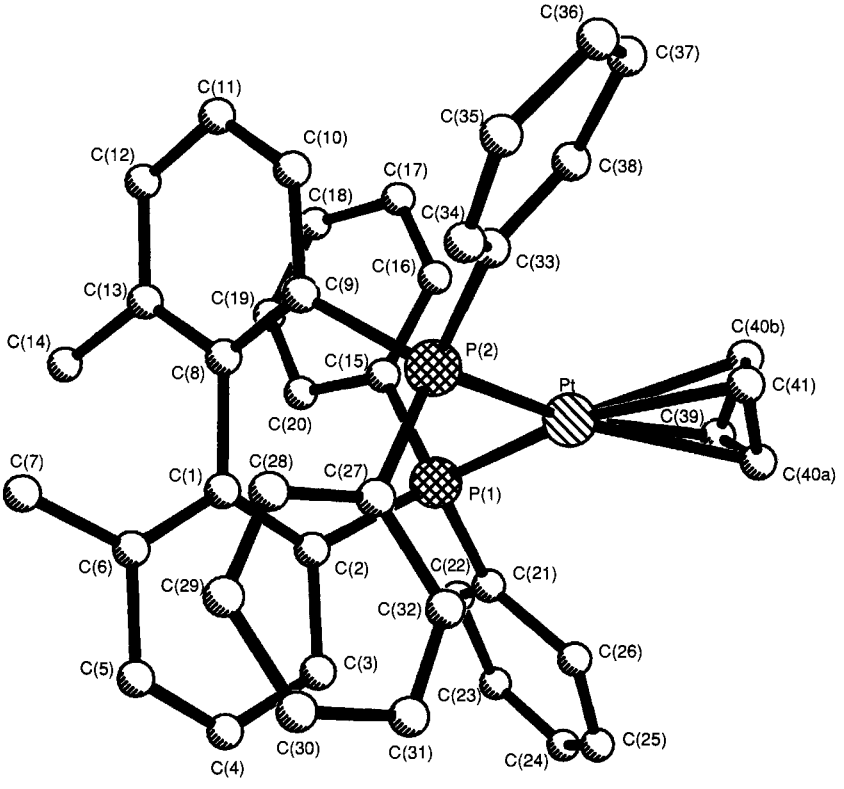

Fig. 4. *Structure of [Pt{(R)-biphemp}(allyl)]$^+$* (cation of **5**) *with arbitrary atom-numbering scheme*

Table 1. *Selected Structural Parameters for [Pd{(R)-biphemp}(allyl)]ClO$_4$* (**4**), [Pt{(R)-*biphemp*}(*allyl*)]ClO$_4$ (**5**), *and [Ni{(R)-biphemp}(2-methylallyl)]ClO$_4$* (**6**)

		4 (M = Pd)	**5** (M = Pt)	**6** (M = Ni)
Bond lengths [Å]	M–P(1)	2.304 (02)	2.277 (02)	2.201 (08)
	M–P(2)	2.316 (02)	2.279 (03)	2.184 (07)
	P(1)–C(2)	1.846 (07)	1.824 (11)	1.820 (26)
	P(1)–C(15)	1.800 (07)	1.826 (09)	1.810 (24)
	P(1)–C(21)	1.805 (07)	1.791 (11)	1.796 (25)
	P(2)–C(9)	1.842 (08)	1.836 (10)	1.835 (23)
	P(2)–C(27)	1.807 (08)	1.825 (11)	1.829 (30)
	P(2)–C(33)	1.801 (08)	1.816 (10)	1.836 (24)
	C(1)–C(2)	1.399 (10)	1.403 (15)	1.448 (35)
	C(1)–C(8)	1.476 (11)	1.532 (13)	1.532 (36)
	C(8)–C(9)	1.447 (11)	1.420 (14)	1.454 (35)
	M–C(39)	2.198 (07)	2.203 (11)	2.034 (32)
	M–C(40a)[a])	2.181 (18)	2.184 (23)	2.079 (26)
	M–C(40b)[a])	2.160 (18)	2.141 (27)	–
	M–C(41)	2.215 (10)	2.218 (12)	2.028 (24)
	C(39)–C(40a)[a])	1.314 (20)	1.337 (26)	1.337 (41)
	C(39)–C(40b)[a])	1.279 (21)	1.391 (30)	–
	C(41)–C(40a)[a])	1.348 (24)	1.449 (27)	1.265 (35)
	C(41)–C(40b)[a])	1.401 (20)	1.395 (29)	–
Bond angles [°]	P(1)–M–P(2)	95.7 (1)	95.4 (1)	99.1 (3)
	M–P(1)–C(2)	109.9 (2)	111.2 (3)	110.5 (9)
	M–P(1)–C(15)	113.8 (2)	113.5 (3)	110.8 (8)
	M–P(1)–C(21)	113.7 (3)	112.8 (4)	116.0 (9)
	M–P(2)–C(9)	110.6 (2)	111.4 (3)	116.1 (7)
	M–P(2)–C(27)	113.8 (3)	114.9 (4)	111.8 (10)
	M–P(2)–C(33)	113.9 (3)	113.6 (5)	111.6 (7)
	C(2)–P(1)–C(15)	108.8 (3)	107.7 (5)	112.1 (12)
	C(2)–P(1)–C(21)	103.7 (3)	103.3 (5)	103.0 (12)
	C(9)–P(2)–C(27)	110.2 (3)	108.6 (5)	105.7 (11)
	C(9)–P(2)–C(33)	103.6 (4)	102.9 (5)	103.8 (10)
Torsion angles [°]	M–P(1)–C(2)–C(1)	73.6	72.7	69.2
	P(1)–C(2)–C(1)–C(8)	4.0	5.5	12.6
	C(2)–C(1)–C(8)–C(9)	–77.1	–77.8	–84.6
	C(1)–C(8)–C(9)–P(2)	14.0	16.7	23.4
	C(8)–C(9)–P(2)–M	70.0	68.5	59.0
	C(9)–P(2)–M–P(1)	–42.8	–42.4	–34.2
	P(2)–M–P(1)–C(2)	–34.2	–33.7	–41.4
Interplanar angles [°][b])	[C(1–6)]/[C(8–13)]	77.4	77.0	76.4
	[C(1–6)]/[C(27–32)]	13.3	14.1	11.8
	[C(1–6)]/[C(21–26)]	101.9	102.1	112.6
	[(C(8–13)]/[C(15–20)]	19.9	20.4	31.8
	[(C(8–13)]/[C(33–38)]	107.7	108.3	118.7
	[(C(15–20)]/[C(21–26)]	54.7	54.8	65.8
	[(C(27–32)]/[C(33–38)]	62.8	63.5	68.0

[a]) C(40) disordered in two positions in complexes **4** and **5**.

[b]) Angles between least-squares planes through the atoms indicated.

(2 × 2.28(0.3) Å) to Ni (2.18(0.7), 2.20(0.8) Å). All values comply well with literature precedents.

The metal and the two P-atoms are occupying contiguous positions in a seven-membered chelate ring that is held in a rigid chiral conformation. The chirality of this conformation (λ-skew-(v) [9]) is, of course, established by the chirality of the biphemp ligand. The ring geometry of **6** differs slightly from that of **4** and **5**. The shorter Ni–P bonds require a slightly (+4°) larger (P–Ni–P) angle. A local deformation around C(8)–C(9) occurs in all three structures (most pronounced, however, in **6**) and is attributed to crystal-packing effects. This deformation causes the torsion angles C(1)–C(8)–C(9)–P(2) and C(13)–C(8)–C(9)–P(2) to deviate significantly (up to 23.4°) from planarity. The analogous torsion angles at the opposite backbone ring, C(8)–C(1)–C(2)–P(1) and C(6)–C(1)–C(2)–P(1), are noticeably out of planarity (12.6 and 10.5°) only in structure **6**. The biaryl backbone axis deviates from linearity in all three structures: a line passing through C(1) and C(4) intercepts C(8)–C(11) at an angle of 172.1 (**4**), 172.3 (**5**), and 167.2° (**6**). The interplanar angle (least-squares planes) between the two backbone benzene rings is 77.4 (**4**), 77.0 (**5**), and 76.4° (**6**). The corresponding angle in the free ligand was previously determined (88.7° [3a]). Complexation thus requires only a relatively minor rotational adjustment of the biaryl backbone. The valence geometry at the P-atoms is practically tetrahedral in all three structures and defines the positions of the four Ph–P rings. Two of them (one on each P) are disposed quasi-axially in a near parallel orientation to either one of the backbone benzene rings. Shortest atom distances between these nearly parallel rings range from 3.1 to 3.3 Å, implying effective *van-der-Waals* contacts between them. This attractive interaction is an obvious consequence of metal coordination and was observed in all previously determined crystal structures of biphemp [3] [10] or binap [1] [11] derivatives, not, however, in the free biphemp ligand [3a]. Coordination thus requires a rotation of *ca.* 50° around both the P(2)–C(9) and the P(1)–C(2) bonds. The remaining two Ph–P rings (again one on each P) are disposed quasi-equatorially and then oriented edge-to-face with either one of the backbone benzene rings. Contrary to their geminal neighbors, they can rotate freely around their Ph–P bonds. The Ph orientations observed in the three structures are only slightly different. They remain almost unchanged after relaxation in a molecular-mechanics force field.

The disposition of the four Ph–P rings defines a chiral surface capable of distinguishing the faces of a prochiral substrate. Using standard *van-der-Waals* radii, this surface is estimated to span *ca.* 240 Å^2. It was previously recognized [1c] that the spatial fixation of the two pseudo-axial Ph–P rings effectively inhibits their interconversion to the corresponding pseudo-equatorial positions. This then prevents transitory C_{2v} symmetry of the *van-der-Waals* surface and is considered an intrinsic advantage of binap- or biphemp-type catalysts. The present data fully support that conclusion.

No detailed investigations of the solution behavior of **4**–**6** was carried out. We do, however, expect an arrangement at least similar to that in the crystal environment on the basis of circumstantial NMR evidence. ^{1}H-NMR Data are typical for η^3-bonded allyl: the central H-atom appears between 5.4 and 6.0 ppm ($CDCl_3$) with a large (*trans*) and a small (*cis*) coupling constant. Separate resonances are observed for the 4 terminal allylic H-atoms indicating the maintenance of an asymmetric environment in solution. This conclusion can also be drawn from the ^{31}P-NMR spectra. The two P-atoms are non-equivalent and appear at slightly different field. The ^{31}P,^{195}Pt-coupling constants observed

for compound **5** (3770 and 3970 Hz) are in a range characteristic for η^3-complexes. Quite in contrast, the ^{1}H-NMR spectra of the precursor complexes **1** and **2** indicate the presence of a dynamic process: The 4 signals of the terminal allylic H-atoms coalesce into 1 broad peak, and the resonance of the central H-atom collapses from a *tt* to a *quint.* with averaged coupling constant. The ^{31}P-resonance is reduced from an *AB* system to a single line. This fluxional behavior is due to the presence of a coordinating counterion and may, as supported by extensive literature analogies [12], be attributed to a Cl^--assisted equilibration of the π-allyl ligand *via* transient σ-species (π-σ-π rearrangement).

3. Discussion. – The X-ray analyses presented above represent the first structural information on group-VIIIc-metal complexes bearing axially dissymmetric diphosphine ligands. They complement previous data [3] [9–11] on a number of related Rh and Ru complexes. The crystal structure of [Rh{(*R*)-biphemp}(nbd)]PF_6 (nbd = norbornadiene) [10] is the closest literature precedent available. A comparison of this structure with its group-VIII neighbor **4** reveals a fairly similar overall picture. An interpretation of the structural differences is, however, not straightforward due to their different crystal-packing arrangements. The Rh complex clearly has a less deformed backbone and a slightly different torsional geometry of the chelate ring: a smaller (6°) valence angle at Rh is accompanied by a smaller (5°) interplanar backbone angle. These subtle differences do, however, translate into sizeable deviations of the Ph–P ring positions (r.m.s.d. of the biphemp ligand, 0.77 Å).

The usefulness of crystal structures (together with kinetic data to correctly extrapolate from ground to transition state) for the understanding of asymmetric catalysis was repeatedly emphasized [13]. For instance, a comparative evaluation of a number of bis(phosphine)rhodium complexes allowed to establish a model of the chirality transfer in asymmetric hydrogenations [14]. Even before kinetic data had become available, empirical rules concerning the sense of induction were formulated on the basis of crystal data [15]. In an analogous fashion, we expect the present information to contribute to an understanding of the stereochemistry of reactions catalyzed by these types of complexes. This seems to be all the more desirable, since applications of [Pd(binap)]-based catalyst systems have so far incurred widely varying stereochemical results. Moderate to high ee's were realized for a 1,4-addition of disilanes to enones (74–92%) [16] and for an intramolecular *Heck*-type alkenylation (up to 80%) [17]. An allylic substitution reaction (ee 47%) [18] and a hydrocyanation (ee 40%) [19] proceeded less satisfactorily. Our own efforts in this area [6] met with moderate success: tocopherol building blocks of up to 56% ee could be obtained in an intramolecular allylic substitution catalyzed by **1** or **4**. On the other hand, a cross coupling reaction catalyzed by [$NiBr_2$\{(*R*)-biphemp\}] produced alkanes with 65–95% ee [20]. To the best of our knowledge, no applications for Pt-based catalysts have been reported yet.

We are grateful to our colleagues Dr. *W. Arnold*, *A. Bubendorf*, *A. Dirscherl*, *W. Meister*, *Y. Mercadal*, and Mrs. *J. Kohler* for conducting spectroscopic and combustion analyses. We wish to thank *B. Weber* for experimental assistance and Dr. *R. K. Müller* for the support of this project.

Experimental Part

General. Reactions were conducted in oven-dried glassware in an atmosphere of dry Ar. Solvents were distilled from CaH_2 immediately prior to use. Drying *in vacuo* refers to 0.001 mbar at 60–80° for 24 h. CD Spectra: *Jobin-Yvon-185* dichrograph; 0.1-mm cuvets; recording between 207 and 400 nm, at r.t.; sample concentration 1–1.5 mM in MeCN; data quoted as $\Delta\varepsilon$. IR Spectra: *Nicolet-170-SX-FT-IR* spectrometer; KBr pellets; in cm^{-1}. NMR Spectra: *Bruker AC-250*; at 250 (^1H), 62.9 (^{13}C), and *Bruker AM-400* at 162 (^{31}P) MHz; TMS as internal standard (^1H,^{13}C) 85% H_3PO_4 as external standard (^{31}P); chemical shifts in ppm, coupling constants J in Hz. FAB-MS: *Finnigan MAT-90* with Xe (6 keV) as reaction gas; 3-nitrobenzyl alcohol matrix; excellent agreement between observed and calculated isotope patterns for metal-containing fragments, m/z given for lowest-weight metal isotope observed.

[(R)-(6,6'-Dimethyl-1,1'-biphenyl-2,2'-diyl)bis(diphenylphosphine)-P,P'](η^3-prop-2-enyl)palladium Chloride (**1**). Acetone (0.8 ml) was added to a solid mixture of (*R*)-biphemp (110 mg, 0.2 mmol) and bis[(allyl)palladium chloride] (*Aldrich*; 37 mg, 0.1 mmol) (→lemon-yellow soln., then precipitate). Stirring was continued for 30 min and the resulting suspension set aside at 0° for 1 h. The solvent was removed and the residue washed with several portions of ice-cold acetone and dried *in vacuo*: 96 mg (65%) of slightly yellow crystals. M.p. > 180°. CD: 220 (−47, neg.max), 236 (0), 240 (+8, pos.max), 250 (0), 258 (−3, neg.max), 268 (0), 297 (+18, pos.max), 340 (0). IR: 1477*m*, 1435*s*, 1099*m*, 998*w*, 749*s*, 697*s*, 542*m*, 503*s*, 469*m*. ^1H-NMR ($CDCl_3$): 7.7–6.74 (*m*, arom. H); 5.92 (*quint.*, $J = 11$, CH_2CHCH_2); 3.8 (br. *s*, CH_2CHCH_2); 1.44 (*s*, 2 Me). ^{31}P-NMR (DMSO): 22.46 (*s*). MS: 695 ([^{104}Pd (biphemp)(allyl)]$^+$).

[(R)-(6,6'-Dimethyl-1,1'-biphenyl-2,2'-diyl)bis(diphenylphosphine)-P,P'](η^3-prop-2-enyl)platinum Chloride (**2**). Acetone (2.5 ml) was added to a solid mixture of (*R*)-biphemp (220 mg, 0.4 mmol) and tetrakis[(allyl)platinum chloride] (109 mg, 0.1 mmol) [7a]. The resulting suspension was stirred for 24 h and filtered. The solid was washed with acetone (3 × 1 ml) and dried. For purification, the crude material (220 mg) was redissolved in acetone (20 ml), filtered over *Celite*, and the resulting soln. concentrated to *ca.* 2 ml. A small amount of solid material was removed by filtration, and the mother liquor was treated with pentane to precipitate the product: 120 mg (36%) of off-white powder, after drying *in vacuo*. M.p. > 180°. CD: 216 (−31, neg.max), 227 (0), 237 (+14, pos.max), 248 (+9, pos.min), 261 (+13, pos.max), 284 (0), 289 (−1, neg.max), 294 (0). IR: 1477*m*, 1436*s*, 1400*w*, 1100*m*, 999*w*, 749*s*, 698*s*, 546*m*, 505*s*, 476*m*. ^1H-NMR ($CDCl_3$): 7.65–6.73 (*m*, arom. H); 5.52 (*quint.*, with ^{195}Pt satellites, J(H,H) = 10, J(Pt,H) = 54, CH_2CHCH_2); 3.7–3.3 (br. *s*, CH_2CHCH_2); 1.46 (*s*, 2 Me). ^{31}P-NMR (DMSO): 14.28 (*s*, with ^{195}Pt satellites at 26.2 and 2.38, J(Pt,P) = 3860). MS: 785 ([^{194}Pt (biphemp)(allyl)]$^+$).

[(R)-(6,6'-Dimethyl-1,1'-biphenyl-2,2'-diyl)bis(diphenylphosphine)-P,P'](η^3-prop-2-enyl)palladium Perchlorate (**4**). A soln. of **1** in MeOH (1.5 ml) was prepared from (*R*)-biphemp (220 mg, 0.4 mmol) and bis[(allyl)palladium chloride] (74 mg, 0.2 mmol) as described above. A soln. of $LiClO_4$ (212 mg, 2 mmol) in MeOH (1 ml) was added dropwise. A colorless precipitate appeared immediately, and stirring was continued overnight. Too fine to be filtered, the precipitate was dissolved by the addition of $CHCl_3$. The resulting soln. was washed with H_2O, dried (Na_2SO_4), and evaporated. The residue was crystallized from acetone to yield, after drying *in vacuo*: 280 mg (88%) of **4**. Colorless powder. M.p. > 180°. CD: 219 (−55, neg.max), 235 (0), 240 (+8, pos.max), 249 (0), 258 (−5, neg.max), 279 (0), 297 (+21, pos.max), 352 (0). IR: 1475*m*, 1436*s*, 1095*s*, 995*m*, 747*s*, 698*s*, 621*m*, 542*m*, 502*m*, 489*m*. ^1H-NMR (DMSO): 7.75–6.8 (*m*, arom. H); 6.03 (*tt*, $J = 7$, 14, CH_2CHCH_2); 4.13, 2.93 (2*m*, 2 H_{trans} of CH_2CHCH_2); 4.01, 3.68 (2*t*, 2 H_{cis} of CH_2CHCH_2); 1.50, 1.44 (2*s*, 2 Me). ^1H-NMR ($CDCl_3$): 7.64–6.72 (*m*, arom. H); 5.86 (*tt*, $J = 7$, 14, CH_2CHCH_2); 4.08–3.95 (*m*, 1 H_{cis}, 1 H_{trans} of CH_2CHCH_2); 3.73 (*m*, 1 H_{cis} of CH_2CHCH_2); 2.84 (*m*, 1 H_{trans} of CH_2CHCH_2); 1.48, 1.40 (2*s*, 2 Me). ^{13}C-NMR (DMSO): 139–126 (arom. C); 123.6 (CH_2CHCH_2); 80.5, 73.1 (2*dd*, J(P,C) = 9, 23, CH_2CHCH_2); 19.3 (2 Me). ^{31}P-NMR (DMSO): 22.78, 22.40 (*AB*, J(P,P) = 50). MS: same as for **1**. Anal. calc. for $C_{41}H_{37}ClO_4P_2Pd$ (797.54): C 61.75, H 4.68; found: C 61.62, H 4.78.

[(R)-(6,6'-Dimethyl-1,1'-biphenyl-2,2'-diyl)bis(diphenylphosphine)-P,P'](η^3-prop-2-enyl)platinum Perchlorate (**5**). A suspension of **2** in acetone (8 ml) was prepared from (*R*)-biphemp (507 mg, 0.92 mmol) and tetrakis[(allyl)platinum chloride] (250 mg, 0.23 mmol) [7a] as described above. A soln. of $LiClO_4$ (636 mg, 6 mmol) in acetone (5 ml) was introduced dropwise (→white precipitate). After 2 h, the solid was collected on a filter, washed with acetone (10 ml) followed by pentane (5 ml), and dried *in vacuo*: 713 mg (87%) of colorless powder. M.p. > 180°. CD: 214 (−45, neg.max), 230 (0), 240 (+26, pos.max), 258 (+19, sh), 284 (0), 287 (−1, neg.max), 293 (0), 298 (+2, pos.max), 330 (0). IR: 1478*m*, 1437*s*, 1096*s*, 749*m*, 697*s*, 622*m*, 545*m*, 505*s*, 476*m*. ^1H-NMR ($CDCl_3$): 7.62–6.7 (*m*, arom. H); 5.61–5.20 (*m*, CH_2CHCH_2); 3.81, 3.46, 3.43, 2.32 (4*m*, CH_2CHCH_2); 1.49, 1.43 (2*s*, 2 Me). ^{13}C-NMR (DMSO): 139.7–125.9 (arom. C); 119.1 (CH_2CHCH_2); 73.2, 64.5 (2*dd*, with ^{195}Pt satellites, J(P,C) = 7, 31, J(Pt,C) = 90, CH_2CHCH_2); 19.8 (2 Me). ^{31}P-NMR (DMSO): 14.5, 13.8 (*AB*, J(P,P) = 17, with ^{195}Pt satellites at 26.1 (*s*), 2.8 (*d*, J(P,P) = 17), and 1.6 (*d*, J(P,P) = 17); J(Pt,P) = 3770, 3970). MS: same as for **2**. Anal. calc. for $C_{41}H_{37}ClO_4P_2Pt$ (886.23): C 55.57, H 4.21; found: C 55.29, H 4.31.

[(R)-(6,6'-Dimethyl-1,1'-biphenyl-2,2'-diyl)bis(diphenylphosphine)-P,P'](η³-2-methylprop-2-enyl)nickel Perchlorate (**6**). A suspension of (*R*)-biphemp (220 mg, 0.4 mmol) in benzene (3 ml) was added to a soln. (0.2M, 3 ml) of bis[(2-methylallyl)nickel bromide] [7b] in benzene. The resulting, dark-red soln. was stirred for 5 min and treated dropwise with a soln. of $LiClO_4$ (400 mg, 3.7 mmol) in acetone (3 ml). Stirring was continued for 2 h and the mixture partitioned between H_2O and AcOEt. The org. layer was washed with H_2O, dried (Na_2SO_4), and evaporated. The residual solid was dissolved in CH_2Cl_2 (2 ml), and the product was precipitated from that soln. by the addition of Et_2O (30 ml): 260 mg (85%), after drying *in vacuo*. M.p. > 180°. CD: 219 (−62, neg.max), 243 (0), 251 (+4, sh), 272 (+12, pos.max), 285 (+9, pos.min), 302 (+16, pos.max), 331 (0). IR: 1481*m*, 1436*s*, 1381*w*, 1097*s*, 997*m*, 748*s*, 697*s*, 622*m*, 549*m*, 503*s*, 470*m*. ^{1}H-NMR ($CDCl_3$): 7.7–6.75 (*m*, arom. H); 3.60, 3.20, 2.32 (3*m*, $CH_2C(Me)CH_2$); 1.92 (*s*, $CH_2C(Me)CH_2$); 1.42, 1.37 (2*s*, 2 arom. Me). ^{1}H-NMR (DMSO): 7.82–6.84 (*m*, arom. H); 3.70, 3.25, 3.11, 2.43 (4*m*, $CH_2C(Me)CH_2$); 1.91 (*s*, $CH_2C(Me)CH_2$); 1.41, 1.39 (2*s*, 2 arom. Me). ^{13}C-NMR (DMSO): 139.8–125.9 (arom. C, $CH_2C(Me)CH_2$); 76.4, 69.3 (2*d*, $J(P,C) = 15$, $CH_2C(Me)CH_2$); 22.7 ($CH_2C(Me)CH_2$); 19.6 (2 arom. Me). ^{31}P-NMR (DMSO): 28.5, 26.6 (*AB*, $J(P,P) = 24$). MS: 663 ([^{58}Ni(biphemp)(2-methylallyl)]$^+$). Anal. calc. for $C_{42}H_{39}ClNiO_4P_2$ (763.88): C 66.04, H 5.15; found: C 66.10, H 5.36.

X-Ray Analysis of Compounds **4–6**. Crystal data: see *Table 2*. Data were collected on a *Nicolet-R3m* four-circle diffractometer fitted with a graphite monochromator and a *LT1*-cooling apparatus. Crystals were mounted in

Table 2. *X-Ray Structure Determination of Complexes* **4–6**

	4	**5**	**6**
Crystal data			
Chemical formula	$C_{41}H_{37}ClO_4P_2Pd$	$C_{41}H_{37}ClO_4P_2Pt$	$C_{42}H_{39}ClNiO_4P_2$
Crystallization solvent	MeCN	MeCN/EtOH	MeCN/EtOH
Color, habit	colorless, prismatic	colorless, prismatic	colorless, prismatic
Crystal size [mm]	0.2 × 0.52 × 0.4	0.28 × 0.28 × 0.34	0.17 × 0.17 × 0.5
Crystal system	orthorhombic	orthorhombic	orthorhombic
Space group	$P2_12_12_1$	$P2_12_12_1$	$P2_12_12_1$
Unit-cell dimensions [Å]			
a	10.845(2)	10.851(5)	10.039(2)
b	18.707(3)	18.702(9)	19.059(5)
c	17.883(3)	17.888(8)	19.527(3)
Volume [Å^3]	3628(3)	3630(31)	3736(13)
Z	4	4	4
Formula weight	797.5	886.2	763.8
Density (calc.) [Mg/m^3]	1.451	1.621	1.358
Absorption coefficient [mm^{-1}]	0.714	4.068	0.718
F(000)	1632	1670	1592
Data collection			
Radiation	MoK_α ($\lambda = 0.7107$)	MoK_α ($\lambda = 0.7107$)	MoK_α ($\lambda = 0.7107$)
Temperature [K]	293	183	293
2 Θ Range	0–56	0–56	0–56
Scan type	ω	ω	ω
Scan speed [°/min]	3.91–14.65	2.7–10.0	2.6–10.0
Scan range (ω)	1.11	1.2	1.7
Independent reflexions	8760 (*hkl* and *hk-l*)	4933	5037
Observed reflexions ($F > 5.0\ \sigma(F)$)	5580	3467	1646
Absorption correction	face-indexed-numerical	face-indexed-numerical	none
Solution and refinement			
Solution	heavy-atom method	direct methods	direct methods
Number of parameters	426	421	211
Final *R* index (obs. data)	5.39	4.37	9.29
Absolute structure *p*[a])	0.97(10)	1.09(3)	1.12(2)

[a]) *p* = Coefficient, which multiplies the imaginary component of the atomic scattering factor.

sealed capillaries containing a drop of mother liquor. Remaining parameters: *Table 2*. Solution and refinement: All calculations were carried out with the SHELXTL PLUS package of the *R3m* system. Refinement method: full-matrix least-squares; quantity minimized: $\Sigma w(F_o - F_c)^2$; H-atoms: riding model, fixed anisotropic U; weighting scheme, $w^{-1} = \sigma^2(F) + 0.0010F^2$; remaining parameters: *Table 2*. Coordinates and thermal parameters were deposited with the *Crystallographic Data Centre*, Cambridge, University Chemical Lab., Cambridge CB2 1EW, UK.

REFERENCES

[1] Reviews: a) R. Noyori, H. Takaya, *Acc. Chem. Res.* **1990,** *23,* 345; b) H. Takaya, T. Ohta, K. Mashima, R. Noyori, *Pure Appl. Chem.* **1990,** *62,* 1135; c) S. Otsuka, K. Tani, *Synthesis* **1991,** 665.

[2] S-I. Inoue, H. Takaya, K. Tani, S. Otsuka, T. Sato, R. Noyori, *J. Am. Chem. Soc.* **1990,** *112,* 4897.

[3] a) R. Schmid, M. Cereghetti, B. Heiser, P. Schönholzer, H-J. Hansen, *Helv. Chim. Acta* **1988,** *71,* 897; b) R. Schmid, J. Foricher, M. Cereghetti, P. Schönholzer, *ibid.* **1991,** *74,* 370.

[4] R. Schmid, H.-J. Hansen, *Helv. Chim. Acta* **1990,** *73,* 1258.

[5] B. Heiser, E. A. Broger, Y. Crameri, *Tetrahedron: Asymmetry* **1991,** *2,* 51.

[6] A. Knierzinger, M. Scalone, to *Hoffmann La-Roche AG*, EP 392389, 1990.

[7] a) J. Lukas, *Inorg. Synth.* **1974,** *15,* 75; b) M. F. Semmelhack, P. M. Helquist, *Org. Synth.* **1972,** *52,* 115.

[8] Data collections: a) P. M. Maitlis, P. Espinet, M. J. H. Russell, in 'Comprehensive Organometallic Chemistry', Eds. G. Wilkinson, F. G. A. Stone, and E. W. Abel, Pergamon Press, Oxford, 1982, Vol. 6, pp. 385; b) F. R. Hartley, *ibid.*, pp. 714; c) P. W. Jolly, *ibid.*, pp. 145.

[9] K. Kashiwabara, K. Hanaki, J. Fujita, *Bull. Chem. Soc. Jpn.* **1980,** *53,* 2275.

[10] G. Svensson, J. Albertsson, T. Frejd, T. Klingstedt, *Acta Crystallogr., Sect. C* **1986,** *42,* 1324.

[11] a) M. T. Ashby, M. A. Khan, J. Halpern, *Organometallics* **1991,** *10,* 2011; b) N. W. Alcock, J. M. Brown, J. J. Pérez-Torrente, *Tetrahedron Lett.* **1992,** 389; c) K. Mashima, K. Kusano, T. Ohta, R. Noyori, H. Takaya, *J. Chem. Soc., Chem. Commun.* **1989,** 1208; d) T. Ohta, H. Takaya, R. Noyori, *Inorg. Chem.* **1988,** *27,* 566; e) K. Toriumi, T. Ito, H. Takaya, *Acta Crystallogr., Sect. B* **1982,** *38,* 807.

[12] a) M. Oslinger, J. Powell, *Can. J. Chem.* **1973,** *51,* 274; b) H. C. Clark, C. R. Jablonski, *Inorg. Chem.* **1975,** *14,* 1518; c) H. C. Clark, M. J. Hampden-Smith, H. Ruegger, *Organometallics* **1988,** *7,* 2085.

[13] Reviews: a) H. B. Kagan, in 'Comprehensive Organometallic Chemistry', Eds. G. Wilkinson, F. G. A. Stone, and E. W. Abel, Pergamon Press, Oxford, 1982, Vol. 8, pp. 463; b) V. A. Pavlov, E. I. Klabunovskii, Yu. T. Struchkov, A. A. Voloboev, A. I. Yanovsky, *J. Mol. Catal.* **1988,** *44,* 217.

[14] a) W. S. Knowles, *Acc. Chem. Res.* **1983,** *16,* 106; b) J. M. Brown, P. L. Evans, *Tetrahedron* **1988,** *44,* 4905; c) S. Sakuraba, T. Morimoto, K. Achiwa, *Tetrahedron: Asymmetry* **1991,** *2,* 597.

[15] K. E. Koenig, M. J. Sabacky, G. L. Bachmann, W. C. Christopfel, H. D. Barnstorff, R. B. Friedman, W. S. Knowles, B. R. Stults, B. D. Vineyard, D. J. Weinkauff, *Ann. New York Acad. Sci.* **1980,** *333,* 16.

[16] T. Hayashi, Y. Matsumoto, Y. Ito, *J. Am. Chem. Soc.* **1988,** *110,* 5579.

[17] Y. Sato, M. Sodeoka, M. Shibasaki, *Chem. Lett.* **1990,** 1953.

[18] J. P. Genet, S. Grisoni, *Tetrahedron Lett.* **1988,** 4543.

[19] M. Hodgson, D. Parker, R. J. Taylor, G. Ferguson, *Organometallics* **1988,** *7,* 1761.

[20] G. Consiglio, A. Indolese, *Organometallics* **1991,** *10,* 3425.